

UVA/Vis induced nitrous acid formation on polyphenolic films exposed to gaseous NO₂

Supporting material

Yulia Sosedova, Aurélie Rouvière, Thorsten Bartels-Rausch and Markus Ammann

ESI Section I. Simulation of the temporal evolution of [NO₂], [HONO], [ArNO₂]_s and [ArO•]_s

For the well-mixed conditions in the CWFT and for the beginning of the reaction, assuming diffusion of NO₂ into the underlying film bulk is too slow in comparison to the surface reaction, the HONO formation rate R_{HONO} and the overall NO₂ loss L_{NO_2} (molecule m⁻² s⁻¹) are approximated by the following mass balance equations:

$$R_{\text{HONO}} = k_{s1} \times N_s \times \theta_{\text{NO}_2} \times [\text{ArOH}]_s \quad \text{eq. 1}$$

$$L_{\text{NO}_2} = (k_{s1}[\text{ArOH}]_s + k_{s2}[\text{ArO}^\bullet]_s) \times N_s \times \theta_{\text{NO}_2} \quad \text{eq. 2}$$

$$L_{\text{NO}_2} = R_{\text{HONO}} + R_{\text{ArNO}_2} \quad \text{eq. 2a}$$

where k_{s1} and k_{s2} are the second-order rate constants (m² molecule⁻¹ s⁻¹) for the surface reactions of absorbed NO₂ with the substituted phenol ArOH (gentisic or tannic acid) and the phenoxy radical ArO•, respectively, θ_{NO_2} is the NO₂ molecules surface coverage, N_s is the number of adsorption sites on the surface (molecule m⁻²), $[\text{ArOH}]_s$ and $[\text{ArO}^\bullet]_s$ are the surface concentrations (molecule m⁻²) of the reactive parent molecules (or functional groups) and the phenoxy radical, respectively. The rate of nitro product formation, R_{ArNO_2} (molecule m⁻² s⁻¹), has been introduced in eq. 2a in order to keep up with the mass balance. Similarly, the rate of the phenoxy intermediate ArO• formation, R_{ArO} (molecule m⁻² s⁻¹), is expressed *via* the corresponding mass balance equation:

$$R_{\text{ArO}} = (k_{s1}[\text{ArOH}]_s - k_{s2}[\text{ArO}^\bullet]_s) \times N_s \times \theta_{\text{NO}_2} \quad \text{eq. 3}$$

$$R_{\text{ArO}} = R_{\text{HONO}} - R_{\text{ArNO}_2} \quad \text{eq. 3a}$$

We used eqs. 1–3 to simulate the temporal evolution of the gas-phase concentrations of NO₂ and HONO and the surface concentrations of the nitro product [ArNO₂]_s and of the phenoxy radical. The following initial concentrations were chosen to simulate NO₂ uptake on the TA surface in Fig. 1a: [NO₂]₀ = 33 ppbv, [HONO]₀ = 0, [ArO•]_s = 0. Note that during the simulations, θ_{NO_2} was not affected by the reaction and we kept in mind that k_{s1} , N_s and initial $[\text{ArOH}]_s$ are inter-dependent parameters. We assumed that K_{NO_2} is similar for both coatings and fixed its value in our model to 8.1×10^{-19} m³ molecule⁻¹. In Fig. 1, the values $k_{s1} = 3 \times 10^{-23}$ and $k_{s2} = 6 \times 10^{-21}$ m² molecule⁻¹ s⁻¹, $N_s = 3.2 \times 10^{18}$ molecule m⁻² and $[\text{ArOH}]_s = 3.2 \times 10^{17}$ molecule m⁻² were used in model simulations (red lines) to match both the initially observed HONO formation and NO₂ loss under dark conditions, and the first-order decay kinetics observed for the HONO formation rate, with a first-order rate constant of 6.3×10^{-5} s⁻¹. The latter is driven by the consumption of the reactive molecules (ArOH) in the coating. Similar temporal evolution of HONO formation on a TA coating with MB addition and on GA coatings with and without MB addition was simulated.

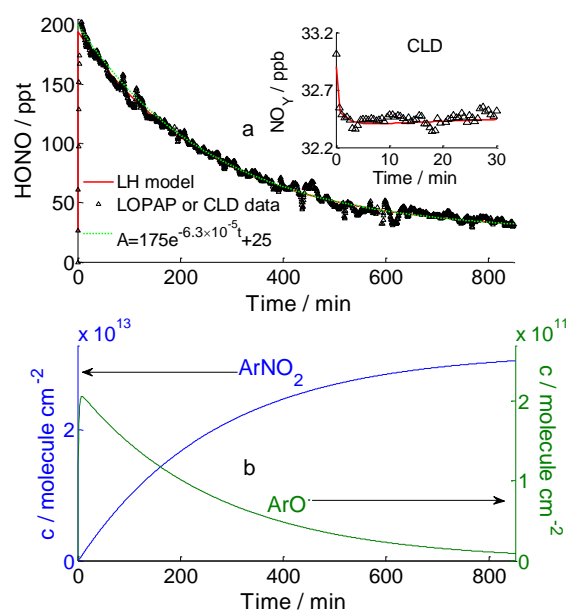


Fig. 1 (a) Typical experiment on HONO formation upon NO_2 (33 ppbv) uptake on a TA coating in the dark: LOPAP and CLD (inset) data are shown with triangles and simulated with the LH model described in the text (red lines). The dashed green line represents a single exponential decay. (b) Simulated surface concentrations of the ArNO_2 product and ArO^* intermediate for a gas residence time in the tube of 0.4 s and with parameters as given in text.

The values of N_s used to simulate NO_2 uptake and HONO formation on GA and TA coatings, as well as on solid anthrarobin [Arens et al., 2002] exceeded the estimated surface density of aromatic rings that was proposed to be a rough approximation for N_s , since aromatic rings could serve as adsorption sites for NO_2 via formation of a charge transfer complex.[Li et al., 1998] The value $N_s = 3.2 \times 10^{18} \text{ molecules m}^{-2}$ required to bring the data in agreement with the simulation (Fig. 1) exceeds the predicted upper limit of about $1.5 \times 10^{18} \text{ m}^{-2}$. This might be a consequence of surface roughness as already proposed for the solid anthrarobin on a comparable substrate [Arens et al., 2002]. Visual inspection of the films revealed that those made of GA did not look smooth, with sometimes irregular precipitates, and those made of TA, though they looked rather smooth over small scales, tended to gain glassy appearance and cracks formed easily during the drying procedure. Thus the effective surface area of both types of coatings could be higher than the geometric inner surface of the CWFT, leading to higher than expected concentration of adsorption sites for NO_2 and thus also normalized rates of HONO formation.

ESI Section II. Calculation of the net uptake coefficient for the dark reaction of NO_2

For comparison with other studies, it is useful to calculate the uptake coefficient γ_{NO_2} , a parameter being usually referred to in the atmospheric chemistry literature, which represents the loss rate of gaseous NO_2 species normalized to the gas-kinetic collision rate with the surface:

$$\gamma_{\text{NO}_2} = \frac{4k_{\text{loss}}}{\omega \times [S/V]} \quad \text{eq. 4}$$

where ω is the mean thermal velocity of NO_2 molecules (369 m s^{-1} at 296 K), $[S/V]$ is the surface to volume ratio of the coated-wall flow tube (m^{-1}) and k_{loss} is the pseudo-first rate constant (s^{-1}) for the NO_2 loss from the gas phase and can be obtained from the experiment for the beginning of the reaction (after the reaction time Δt (s)) and $K_{\text{NO}_2}[\text{NO}_2] \ll 1$:

$$k_{\text{loss}} = -\ln \frac{[\text{NO}_2]}{[\text{NO}_2]_0} \times \frac{1}{\Delta t} \quad \text{eq. 5}$$

Thus, the initial NO_2 uptake coefficient in the dark estimated from Fig. 1 is $\gamma_{\text{NO}_2} = 5 \times 10^{-7}$ on the TA coating and 7×10^{-7} on the GA coating. Though thin solid films of pure catechol were nonreactive with NO_2 under dark and low RH conditions [George et al., 2005; Kwamena et al., 2007], an enhanced NO_2 uptake coefficient of 7×10^{-6} on catechol adsorbed on a NaCl substrate at a relative humidity of 30 % was reported recently, leading to the formation of nitro-compounds detected by DRIFTS [Woodill and Hinrichs, 2010].

ESI Section III. Calculation of the reactive uptake coefficient for the dark NO_2 to HONO conversion

In order to compare our results with previous studies, which were focused only on the formation of the gas-phase product, HONO, we also calculated the reaction probability that a gas kinetic collision of an NO_2 molecule leads to the formation of a HONO molecule, γ_{rxn} , by eq. 4 using k_{prod} instead of k_{loss} for the beginning of the reaction:

$$k_{\text{prod}} = -\ln \frac{[\text{NO}_2]_0 - \Delta[\text{HONO}]}{[\text{NO}_2]_0} \times \frac{1}{\Delta t} \quad \text{eq. 6}$$

The resulting γ_{rxn} was $\sim 3 \times 10^{-7}$ for the TA and GA coating and 7 – 8 times higher for the TA and GA coatings with 1 wt.% MB addition (2×10^{-6} and 2.4×10^{-6} , respectively) and decreased with increasing NO_2 concentration. The range of γ_{rxn} obtained is similar to the reported NO_2 dark uptake coefficients of $7 \times 10^{-7} - 2 \times 10^{-6}$ on anthrarobin films¹⁵ and higher than on humic acid surfaces with an upper limit $< 10^{-7}$ [Stemmler et al., 2007]. Lower reactivity of the humic acid coatings in the dark is likely due to the presence of some electron withdrawing groups.

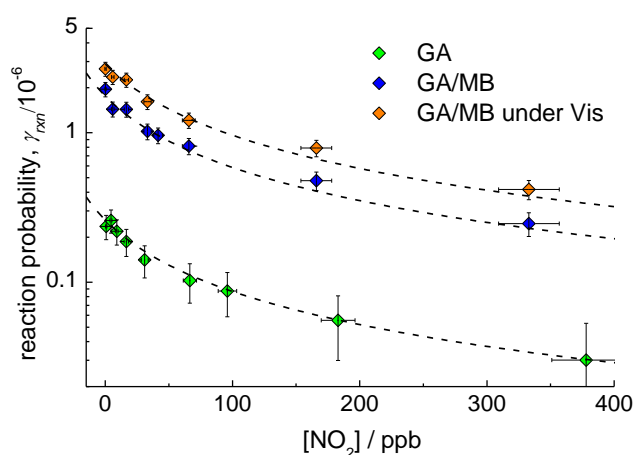


Fig. 2 Reaction probability of the NO_2 uptake leading to HONO formation on GA coating (0.5 mg cm^{-2} GA, 0.05 mg cm^{-2} citric acid) without (green diamonds) and with 1 wt.% MB addition (blue diamonds) in the dark as a function of NO_2 concentration, and on GA coating with 1% MB addition under 7 Vis lamps irradiation (orange diamonds). For model description (dashed lines) see text.

ESI Section IV. Dependence of the reactive uptake coefficient for NO_2 to HONO conversion on the initial $[\text{NO}_2]$

Fig. 2 demonstrates how γ_{rxn} for NO_2 conversion to HONO in the dark and under irradiation decreases with increasing the initial NO_2 concentration, $[\text{NO}_2]$. Eq. 7 describes this dependence for the dark NO_2 uptake within the Langmuir-Hinshelwood model, with $k_{\text{prod}} = 8.7 \times 10^{-2}$ and $1.2 \times 10^{-2} \text{ s}^{-1}$ for HONO formation on the GA coating with and without addition of 1 wt.% MB, respectively and the adsorption equilibrium constant of $K_{\text{NO}_2} = 8.1 \times 10^{-19} \text{ m}^3 \text{ molecule}^{-1}$.

$$\gamma_{\text{rxn}} = \frac{2r}{\omega} \times \frac{k_{\text{prod}}}{1 + K_{\text{NO}_2} [\text{NO}_2]} \quad \text{eq. 7}$$

NO₂ reactive uptake on GA coating with 1 wt.% addition of MB under visible irradiation as a function of [NO₂] is described in Fig. 2 as a sum of the dark and photoenhanced uptake, using model eq. 8 with parameters $k_{\text{eff}} = 5.2 \times 10^{-2} \text{ s}^{-1}$ and $k_{\text{max}} = 0.37 \text{ ppbv s}^{-1}$ per lamp or $4.5 \times 10^{-21} \text{ ppbv s}^{-1}$ per photon $\text{s}^{-1} \text{ m}^2$.

$$\gamma_{\text{rxn}} = \frac{2r}{\omega} \times \left\{ \frac{k_{\text{prod}}}{1 + K_{\text{NO}_2} [\text{NO}_2]} + \frac{k_{\text{eff}}}{1 + \frac{k_{\text{eff}} \times [\text{NO}_2]}{k_{\text{max}} \times [F]}} \right\} \quad \text{eq. 8}$$

Arens, F., L. Gutzwiller, H. W. Gäggeler and M. Ammann. The reaction of NO₂ with solid anthrarobin (1,2,10-trihydroxyanthracene). *Physical Chemistry Chemical Physics* **4**(15): 3684-3690, 2002.

George, C., R. S. Strekowski, J. Kleffmann, K. Stemmler and M. Ammann. Photoenhanced uptake of gaseous NO₂ on solid-organic compounds: a photochemical source of HONO? *Faraday Discussions* **130**: 195-210, 2005.

Kwamena, N. O. A., M. G. Staikova, D. J. Donaldson, I. J. George and J. P. D. Abbatt. Role of the aerosol substrate in the heterogeneous ozonation reactions of surface-bound PAHs. *Journal of Physical Chemistry A* **111**(43): 11050-11058, 2007.

Li, X. Y., S. Y. Shen, Q. F. Zhou, H. J. Xu, D. P. Jiang and A. D. Lu. The gas response behavior of spin-coated phthalocyanine films to NO₂. *Thin Solid Films* **324**(1-2): 274-276, 1998.

Stemmler, K., M. Ndour, Y. Elshorbany, J. Kleffmann, B. D'Anna, C. George, B. Bohn and M. Ammann. Light induced conversion of nitrogen dioxide into nitrous acid on submicron humic acid aerosol. *Atmospheric Chemistry and Physics* **7**: 4237-4248, 2007.

Woodill, L. A. and R. Z. Hinrichs. Heterogeneous reactions of surface-adsorbed catechol with nitrogen dioxide: substrate effects for tropospheric aerosol surrogates. *Physical Chemistry Chemical Physics* **12**(36): 10766-10774, 2010.